

Hyaluronidase-Expressing *Salmonella* Effectively Targets Tumor-Associated Hyaluronic Acid in Pancreatic Ductal Adenocarcinoma

Nancy D. Ebel, Edith Zuniga, Kevin B. Passi, Lukas J. Sobocinski, and Edwin R. Manuel



ABSTRACT

In pancreatic ductal adenocarcinoma (PDAC), the extracellular matrix (ECM) surrounding cancer cells forms a barrier that often limits the ability of chemotherapeutic drugs and cytotoxic immune subsets to penetrate and eliminate tumors. The dense stromal matrix protecting cancer cells, also known as desmoplasia, results from the overproduction of major ECM components such as collagens and hyaluronic acid (HA). Although candidate drugs targeting ECM components have shown promise in increasing penetration of chemotherapeutic agents, severe adverse effects associated with systemic depletion of ECM in peripheral healthy tissues limits their use at higher, more effective doses. Currently, few strategies exist that preferentially degrade ECM in tumor tissue over

healthy tissues. In light of this, we have developed an attenuated, tumor-targeting *Salmonella typhimurium* (ST) expressing functional bacterial hyaluronidase (bHs-ST), capable of degrading human HA deposited within PDAC tumors. Our data show that bHs-ST (i) targets and colonizes orthotopic human PDAC tumors following systemic administration and (ii) is efficiently induced *in vivo* to deplete tumor-derived HA, which in turn (iii) significantly increases diffusion of *Salmonella typhimurium* within desmoplastic tumors. bHs-ST represents a promising new tumor ECM-targeting strategy that may be instrumental in minimizing off-tumor toxicity while maximizing drug delivery into highly desmoplastic tumors.

Introduction

Pancreatic ductal adenocarcinoma (PDAC) is predicted to become the second leading cause of cancer-related death in western countries and, thus, is considered a major public health concern (1). Currently, the approved drug combination of gemcitabine and nanoparticle albumin-bound paclitaxel (Abraxane) and the highly toxic FOLFIRINOX for advanced PDAC have been shown to improve patient survival compared with gemcitabine alone (2, 3). However, these toxic regimens may only extend survival for a matter of months at the expense of decreased quality of life and increased potential for complications later in life (4). The continued lack of early detection methods, poor treatment efficacy, and resistance contribute to a meagre 5-year survival rate (for all stages) of only 7% (5). It is imperative that new agents and combination treatment strategies are developed to improve overall survival for patients with PDAC.

Hyaluronic acid (HA), also known as hyaluronan, is a component of PDAC stroma that is expressed at extremely high levels in the extracellular matrix (ECM), resulting in a biophysical barrier that significantly increases interstitial fluidic pressure, compresses blood vessels, and hinders effective drug delivery (6, 7). While PDAC tumors have the greatest incidence of HA overexpression in patients (>95%), other cancer types such as breast and prostate cancer also express high levels (8, 9), and metastatic lesions have

been found to have similar levels of HA to the primary tumor (10). Thus, agents to degrade tumor-derived HA, and other overexpressed ECM components, to improve drug delivery and efficacy has been an area of extensive research (11–14). Recently, clinical trials with a pegylated form of the human hyaluronidase PH20 (PEGPH20) reported significant increases in progression-free and overall survival when combined with Abraxane and gemcitabine compared with gemcitabine alone (15). However, because hyaluronidase is delivered systemically and activity is not restricted to only tumor tissue, significant adverse events have been observed relating to HA depletion in joints and other organs, requiring lower doses or coadministration with additional agents to minimize these stresses (7, 16, 17). Oncolytic viruses, specifically adenoviruses, encoding human PH20 are among the few agents that can cause tumor-specific ECM degradation (18).

While eukaryotic hyaluronidases have been categorized as “hyaluronidases,” numerous studies have confirmed a broader target range to include degradation of chondroitin, chondroitin sulfates, and collagen (19, 20). While degradation of these additional ECM components in the tumor could be beneficial to maximizing drug delivery to tumor cells, this may further contribute to systemic toxicity as these components are also abundant in nonmalignant, healthy peripheral tissues. Bacterial hyaluronidases (bHs) have long been studied as a cost-effective alternative to bovine and human hyaluronidases, due to greater ease in purification and a single specificity to HA depending on the bHs used (21). Nearly all bHs are expressed by Gram-positive bacteria, which include the genera *Streptococcus*, *Streptomyces*, and *Clostridium* and, like in eukaryotes, act primarily as tissue remodeling or “spreading” factors (22). Although bHs have been purified and shown to have comparable or higher activity than eukaryotic hyaluronidases, similar potential toxicity in humans exists when delivered systemically as bHs, and the bacteria from which they were isolated, are not tumor specific. Several genera of Gram-negative bacteria, however, have been extensively studied for their ability to colonize, replicate in, and regress solid tumors, with attenuated strains of *Salmonella typhimurium* (ST) showing the most promise (23–25). Many studies have

Department of Immuno-Oncology, Beckman Research Institute of the City of Hope, Duarte, California.

Note: Supplementary data for this article are available at Molecular Cancer Therapeutics Online (<http://mct.aacrjournals.org/>).

Corresponding Author: Edwin R. Manuel, Beckman Research Institute of the City of Hope, 1500 East Duarte Road, Duarte, CA 91010. Phone: 626-218-2452, ext. 82452; Fax: 626-930-5492; E-mail: emanuel@coh.org

Mol Cancer Ther 2020;19:706–16

doi: 10.1158/1535-7163.MCT-19-0556

©2019 American Association for Cancer Research.

Targeting Hyaluronan in PDAC using Recombinant *Salmonella*

shown that these attenuated *Salmonella typhimurium* strains are highly tumor specific and are easily cleared from nontumor tissues with ratios from 250:1 to 9,000:1 *Salmonella typhimurium* found within the tumor versus peripheral organs such as the liver (26). Previous work attempting to express human hyaluronidases on the surface of Gram-negative bacteria (i.e., *E. coli*) resulted in auto-display of hyaluronidase with significantly low activity likely due to defective posttranslational modifications and folding (27–29). In contrast, extensive work by Pavan and colleagues describes the successful *E. coli* expression and purification of bHs from *Streptomyces koganeinsis* with activity comparable with or higher than bovine and human hyaluronidases and a unique specificity for only HA (21). However, whether bHs was secreted or auto-displayed in *E. coli* was not determined.

In this study, we have developed and characterized various attenuated *Salmonella typhimurium* strains expressing bHs from *S. koganeinsis* (bHs-ST). We show that attenuated *Salmonella typhimurium* is capable of auto-displaying functional bHs that can effectively degrade purified and tumor-derived HA. We also confirm that bHs-ST, when delivered systemically, is capable of preferentially colonizing orthotopic human PDAC tumors in mice and can cause remarkable degradation of tumor-derived HA resulting in enhanced diffusion of *Salmonella typhimurium* throughout the tumor. This is the first microbial-based, tumor-specific, ECM-degrading strategy that could significantly improve efficacy of therapies for PDAC and other desmoplastic tumor types.

Materials and Methods

Animals and cell lines

NOD/SCID gamma (NSG) mice were obtained from breeding colonies housed at the City of Hope (COH) Animal Research Center and, for all studies, handled according to standard Institutional Animal Care and Use Committee guidelines. The PANC-1 and PC-3 cell lines were obtained from ATCC (CRL1469 and CRL1435) in 2017. Cells were frozen in liquid nitrogen at low passage and used within 20 passages of receipt from ATCC. *Mycoplasma* testing of cell lines was performed following the protocol from Christian Praetorius (Department of Dermatology, University Hospital Carl Gustav Carus, TU Dresden, Germany; BiteSize Bio) derived from Uphoff and Drexler (30). Thawed cells were tested for *Mycoplasma* routinely prior to use in experimentation *in vitro* or prior to implantation in mice. PC-3 cells were maintained in RPMI media containing 10% FBS, 2 mmol/L L-glutamine, and penicillin/streptomycin. PANC-1 cells were maintained at $\leq 80\%$ confluency in DMEM containing 10% FBS, 2 mmol/L L-glutamine, and penicillin/streptomycin.

Salmonella typhimurium strains and generation of bHs-ST

YS1646 was obtained from ATCC (202165). Other attenuated strains were kind gifts obtained from Roy Curtiss III (School of Life Sciences, Arizona State University, Tempe, AZ; χ 8429, χ 8431, and χ 8768), B.A.D Stocker (Department of Microbiology and Immunology, Stanford University School of Medicine, Stanford, CA; SL7207), and Michael Hensel (Abteilung Mikrobiologie, Universität Osnabrück, Osnabrück, Germany; MVP728; refs. 31–35). YS1646 was cultured in modified Luria Broth (LB) media containing MgSO₄ and CaCl₂ in place of NaCl. All other strains were cultured in Miller LB Media (Fisher BioReagents). The *S. koganeinsis* bHs amino acid sequence (UniProt, A0A0U2E2) was used to synthesize an *S. typhimurium* codon-optimized cDNA (Biomatik) inserted in-frame into a 6xHis-EGFP-pBAD bacterial expression vector (kind gift from

Michael Davidson, National High Magnetic Field Laboratory, Department of Biological Science, The Florida State University, Tallahassee, FL; Addgene #54762) using XhoI/EcoRI sites, which removes the EGFP insertion. In-frame insertion of bHs into the pBAD vector adds a 6XHis tag to the N-terminus of the protein and is predicted to generate a membrane-bound bHs upon induction with L-arabinose. This plasmid can be acquired through Addgene, plasmid #134259. χ 8768-LUX was generated using the pAKlux2 plasmid (kind gift from Attila Karsi, Department of Basic Sciences, College of Veterinary Medicine, Mississippi State University, Mississippi State, MS; Addgene #14080). Plasmids were electroporated into *Salmonella typhimurium* strains (1 mm gap cuvettes, settings: 1.8 kV, 186 ohms), spread onto LB plates containing 100 μ g/mL ampicillin, and incubated overnight at 37°C. Glycerol stocks were generated for pBAD-bHs-positive clones identified by colony PCR and restriction digest of plasmid preparations.

Bacterial growth, viability, and analysis of bHs expression

Salmonella typhimurium clones electroporated with pBAD-bHs were cultured in media with or without 2% (w/v) L-arabinose at 37°C, 225 rpm for time intervals ranging from 3–24 hours. Growth kinetics were monitored through absorbance readings at 600 nm (Genesys 30, Thermo Fisher Scientific) every 1–2 hours, up to 24 hours. 6XHis-tagged bHs expression was detected in bacterial lysates by Western blot and localization of bHs was detected by immunofluorescence (IF) using a primary monoclonal mouse anti-6XHis antibody (Protein-tech). For IF, uninduced and induced *Salmonella typhimurium* grown for approximately 3 hours were fixed with 4% paraformaldehyde at room temperature for 30 minutes, and permeabilized with 0.1% Triton-X 100/PBS pH = 7.2 at room temperature for 30 minutes followed by lysozyme (Sigma, 100 μ g/mL final concentration in 5 mmol/L EDTA) at room temperature for 45 minutes. Fixed/permeabilized bacteria were incubated with primary antibody (1:100) for 30 minutes with shaking in a humidified 37°C incubator followed by incubation with FITC-conjugated anti-mouse secondary (1:200, Abcam) and DAPI for 30 minutes with shaking in a humidified 37°C incubator.

Hyaluronan-BSA LB plate and turbidimetric assays

Hyaluronan-BSA LB (HBL) plates for evaluating hyaluronidase activity were generated as previously described. Briefly, LB agar plates containing final concentrations of 0.4 mg/mL HA (Sigma, H-1504), 1% BSA fraction V (Sigma), and 100 μ g/mL ampicillin (Sigma) were used for plating uninduced and induced *Salmonella typhimurium* strains [10^6 colony forming units (CFU)/5 μ L drop] at 37°C for 16–24 hours. Plates were then flooded with 2 N glacial acetic acid. Clear zones were observed against a background of opaque precipitated BSA conjugated to the undigested HA. For turbidimetric quantification of HA degradation in culture media over time, the cetyltrimethylammonium bromide (CTAB) turbidimetric method was used (36). In brief, LB media containing 0.4 mg/mL HA and 100 μ g/mL ampicillin, with or without 2% L-arabinose, was used to culture bHs- *Salmonella typhimurium* strains (2 mL starting volume) over 24 hours at 37°C, 225 rpm. HA content (absorbance) in culture media (100 μ L aliquot) was measured every 2–3 hours by addition of 2.5% CTAB reagent (25 μ L, Sigma) and absorbance read at 600 nm.

Orthotopic and subcutaneous tumor implantation

Previously published methods were used for orthotopic implantation of PANC-1 cells into the pancreas of NSG mice (37). Briefly, while

Ebelt et al.

anesthetized and using sterile techniques, a small incision was made in the skin and peritoneal lining and the pancreas externalized. Using a 27 gauge needle, approximately 2×10^6 PANC-1 cells in a volume of 50 μ L Matrigel (BD Biosciences) were injected into the body of the pancreas. The pancreas was then reinserted into the peritoneal space and inner and outer incisions were closed using absorbable sutures and staples, respectively. Analgesics were administered pre- and postsurgery. For subcutaneous injections, 2×10^6 PANC-1 cells in a volume of 50 μ L Matrigel were injected subcutaneously into the right flank of NSG mice.

Salmonella typhimurium administration, induction, and therapeutic studies in PANC-1 tumor-bearing NSG mice

NSG mice with palpable orthotopic PANC-1 tumors ($>250 \text{ mm}^3$) were intravenously injected with 2.5×10^6 CFU χ 8768-LUX or χ 8768-bHs. For therapeutic studies, mice with subcutaneous PANC-1 tumors ($>150 \text{ mm}^3$) were injected with 2.5×10^6 CFU χ 8768-bHs. Actively growing χ 8768-LUX is constitutively bioluminescent and was used to evaluate χ 8768 colonization of PANC-1 tumors *in vivo* using intravital imaging (LagoX, Spectral Imaging). For all experiments, 2 days after administering χ 8768-bHs, mice were administered 240 mg l-arabinose or PBS intraperitoneally. For gemcitabine treatment, mice were given 40 mg/kg i.p. 2 days later and continued treatment 2 times per week thereafter. Tumor diameters were measured using a digital caliper.

IHC/IF to detect HA, Salmonella typhimurium, and pan-cytokeratin

Prior to incubation with bHs-ST *in vitro*, sections of PANC-1 tumors were deparaffinized and rehydrated. Uninduced and induced χ 8768-bHs (10^8 CFU), PBS, or bovine hyaluronidase (Sigma) were incubated on tissue sections overnight in a humidified 37°C incubator. Following treatment, specimens were incubated with a biotinylated HA-binding protein (HABP, Sigma) at 5 μ g/mL final concentration for 2 hours at 37°C. Slides were then washed, incubated with streptavidin-horse radish peroxidase (HRP) at room temperature for 1 hour, and visualized with a DAB Kit (Vectastain). Hematoxylin and eosin (H&E) and Masson's Trichrome were used for staining. PANC-1 tumor sections, skin, and decalcified joints from NSG mice were treated intravenously with χ 8768-bHs (uninduced and induced). Sections were deparaffinized and rehydrated and stained overnight with 2.5 μ g/mL HABP, 1:100 anti-ST antibody (Santa Cruz Biotechnology, sc-52223), 1:100 anti-pan-cytokeratin (AE1/AE3), or according to H&E and Masson's Trichrome protocols used by the Pathology Research Services Core (COH, Duarte, CA). Streptavidin-PE (Vector), anti-mouse-Cy5 (Invitrogen), or anti-mouse-HRP 1:250 were then used to visualize HA, *Salmonella typhimurium*, or pan-cytokeratin by brightfield or fluorescence microscopy (Zeiss Observer II), in addition to DAPI for visualizing nuclei during fluorescence imaging. Tiling was performed at $5 \times$ or $10 \times$, while higher resolution images for *Salmonella typhimurium*, HA, and DAPI were done at $100 \times$ (oil).

Blood vessel/duct measurements

Ten to 12 fields at $10 \times$ for H&E- and trichrome-stained slides from PANC-1 tumors treated with χ 8768-bHs and induced with l-arabinose or uninduced *in vivo* were imaged using a Leica DMI8 Microscope. In each field, the largest diameter of vessels/ducts containing red blood cells and/or surrounded by collagen were measured using the Leica LasX software. A Mann-Whitney test was performed on values using the Prism 7.2 software from GraphPad.

Results

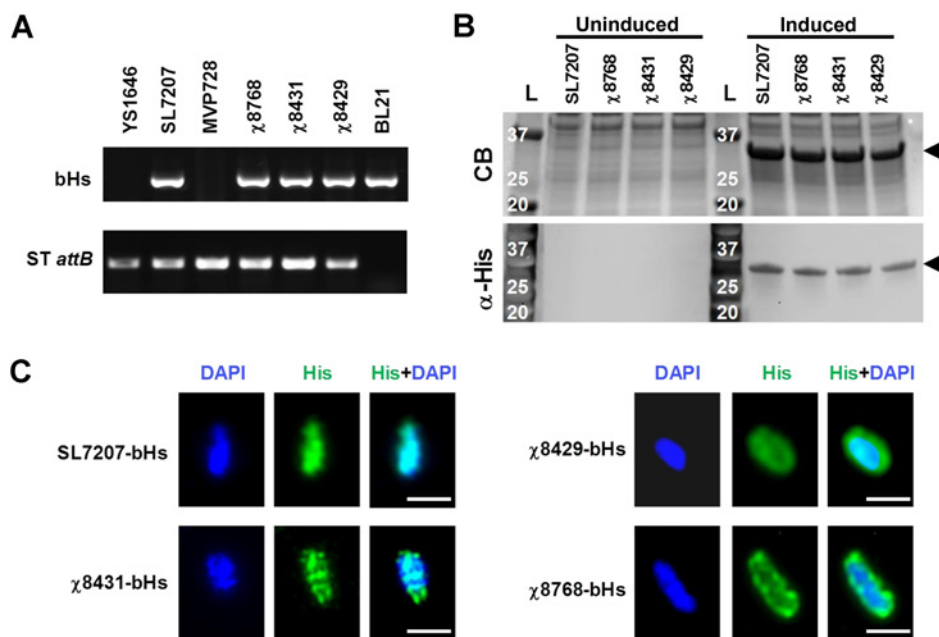
Tightly regulated expression of bHs by attenuated Salmonella typhimurium strains

To circumvent potential toxic effects of constitutive bHs expression on attenuated *Salmonella typhimurium* strains, we employed a tightly regulated inducible expression system. Inducible expression in *Salmonella typhimurium* is possible through the use of a construct containing the P_{BAD} promoter of the araBAD (arabinose) operon and the gene encoding the positive and negative regulator of this promoter, araC (38). A *Salmonella typhimurium* codon-optimized bHs sequence, based on the amino acid sequence of the well-characterized *S. koganezensis* bHs, was synthesized and cloned into a previously described pBAD vector to generate pBAD-bHs (39). A single plasmid preparation of pBAD-bHs was used for electroporation into various attenuated strains of *Salmonella typhimurium* (Supplementary Table S1). Colony PCR was performed for each transformed strain (≥ 8 colonies) to detect for retention of the bHs transgene (Fig. 1A). All ampicillin-resistant colonies examined for YS1646 and MVP728 were completely negative for the bHs transgene in the absence of l-arabinose, suggesting loss of the transgene independent of induced protein expression. Of note, both YS1646 and MVP728 are derived from the same parental strain ATCC 14028. Culturing of pBAD-bHs-positive colonies in uninduced and induced (+2% l-arabinose) conditions, followed by coomassie blue (CB) staining and Western blot analysis of pellet lysates, revealed expression of His-tagged bHs at the correct molecular weight (27 kDa) as well as tight regulation of protein expression (Fig. 1B). No bHs was detected in culture media by CB or Western blot analysis (Supplementary Fig. S1A), suggesting that bHs is not secreted by these *Salmonella typhimurium* strains following induction.

Using HHMTOP, PSORTb, and CellP-Loc subcellular localization prediction tools, bHs is predicted to be anchored to the cytoplasmic membrane at its N-terminus, while the active region (residues 66–247) is localized to the outer membrane/extracellular space (Supplementary Fig. S1B; refs. 40–42). To determine the subcellular location of bHs expressed by the various *Salmonella typhimurium* strains, we performed IF staining to observe the 6XHis-tag fused to the N-terminus of the bHs protein (Fig. 1C). His-tagged bHs expressed by induced χ 8429-bHs and χ 8768-bHs reveals clear bHs localization outside of the bacterial cytoplasm, defined by DAPI staining of genomic DNA. In contrast, bHs expressed by SL7207-bHs, and to a smaller extent in χ 8431-bHs, is localized to the cytoplasm, suggesting impaired transport and formation of inclusion bodies in these attenuated strains. Altogether, these data confirm that expression of the *Salmonella typhimurium* codon-optimized bHs transgene is tightly regulated using an inducible pBAD system and that the expressed bHs protein can be auto displayed on the bacterial surface of certain attenuated *Salmonella typhimurium*.

Growth kinetics and viability of bHs-expressing Salmonella typhimurium strains

While tight regulation of transgene expression is important for minimizing toxicity during initial growth stages, sufficient growth and viability following induction will also be critical to maximizing bHs activity. Thus, we determined growth kinetics of each of the bHs-ST-expressing strains over 24 hours in noninducing and inducing ($\pm 2\%$ l-arabinose) conditions. SL7207 alone is already known to have dramatically reduced growth kinetics compared with wild-type *Salmonella typhimurium*, reaching a maximum optical density (OD) 2–3-fold lower than other attenuated strains (Fig. 2). Under induced conditions, the maximum OD for SL7207-bHs is significantly reduced

Targeting Hyaluronan in PDAC using Recombinant *Salmonella***Figure 1.**

Transgene stability and expression of *Streptomyces koganeinsis* hyaluronidase (bHs) by attenuated *Salmonella typhimurium* strains. **A**, Colony PCR to detect for the bHs transgene contained within an inducible pBAD vector (pBAD-bHs) transformed into indicated *Salmonella typhimurium* strains. Representative colony PCRs shown from ≥ 8 colonies per transformed strain. A positive PCR control using *Salmonella typhimurium*-specific *attB* primers was performed for each colony. *E. coli* (BL21) transformed with pBAD-bHs is used as a positive PCR control for bHs and negative control for *Salmonella typhimurium attB* (*ST attB*). **B**, *Salmonella typhimurium* strains retaining the bHs transgene were cultured in LB media containing 0% (uninduced) or 2% (induced) L-arabinose and cultured for 3 hours at 37°C. Lysates from approximately 5×10^7 CFUs were run on a 4%-20% polyacrylamide gradient gel and subjected to CB staining and Western blot analysis against an amino terminal His-tag fused to bHs (α -His). Predicted bHs size approximately 27 kDa (arrow). L, protein ladder. **C**, *Salmonella typhimurium* strains encoding His-tagged bHs were cultured in LB media containing 2% L-arabinose and immuno-stained (α -His) to determine localization of bHs (green). Nuclei are stained with DAPI (blue). Scale bar, 5 μ m. All data presented are representative of ≥ 3 experiments.

to under 1 (Fig. 2A), whereas other attenuated *Salmonella typhimurium* strains could reach maximum OSs 3-fold higher (Fig. 2B–D). Both, inherently poor growth kinetics of unmodified SL7207, as well as cytoplasmic accumulation of bHs (Fig. 1C), could contribute to the significantly reduced growth kinetics of SL7207-bHs following induction. Interestingly, while $\chi 8431$ -bHs showed mixed localization of bHs by IF, induced growth kinetics were indistinguishable from $\chi 8768$ -bHs and $\chi 8429$ -bHs (Fig. 2D; Supplementary Fig. S1C). These data suggest that $\chi 8768$, $\chi 8431$, and $\chi 8429$ have greater viability upon bHs induction compared with SL7207, which could potentially translate into more extensive HA degradation.

To further investigate bacterial viability after induction, we performed live/dead staining using a mixture of acridine orange (AO) and ethidium bromide (EB), respectively, during log phase (4 hours) and stationary phase (24 hours) of uninduced and induced cultures (43). As shown in Fig. 2E and Supplementary Fig. S1D, the percentage of viable bacterial cells after induction of SL7207-bHs is significantly lower than $\chi 8768$ - and $\chi 8429$ -bHs, as indicated by highly EB-positive SL7207-bHs as early as 4 hours and continuing 24 hours after induction. These results further emphasize the deleterious toxic effects of bHs expression on the viability of attenuated strains such as SL7207 but also highlight *Salmonella typhimurium* strains capable of auto displaying bHs and remaining viable during and long after initiation of induction.

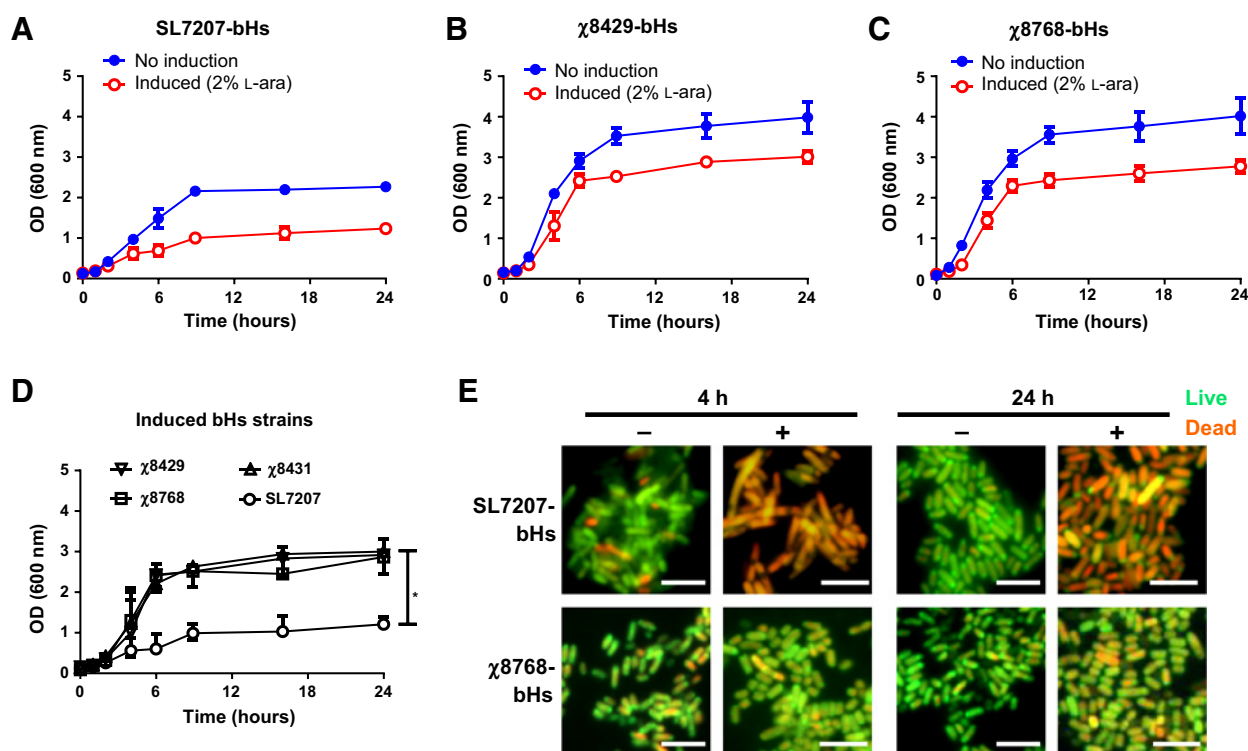
BHs-ST strains degrade purified HA

To test the functionality of bHs expressed by the various attenuated *Salmonella typhimurium* strains, we employed HA agar plate clearing and

liquid culture turbidimetric assays (36). For plate clearing assays, HA and BSA are mixed into LB agar plates (HBL plates). Addition of 2 N acetic acid to HBL plates containing intact HA will form a white precipitate with BSA, while areas of HA degradation will remain clear. BHs-expressing strains were preinduced for 3 hours in LB media containing 0%–4% L-arabinose and then spotted (1×10^8 CFU/5 μ L) onto HBL plates overnight. After flooding HBL plates with 2 N acetic acid, zones of clearing were observed for $\chi 8768$ -, $\chi 8431$ -, and $\chi 8429$ -bHs, but not SL7207-bHs (Fig. 3A). Interestingly, $\chi 8431$ -bHs, which had exhibited intermediate surface display of bHs (Fig. 1C), also demonstrated intermediate HA degradation. These data suggest that *Salmonella typhimurium* strains that efficiently display bHs on their surface and exhibit greater viability are far more effective at degrading pure HA.

To determine the kinetics of HA degradation by the various bHs-ST strains, we cultured each under uninduced and induced conditions in LB media containing HA (0.4 mg/mL) and measured HA content over a 24-hour period using the CTAB turbidimetric method (39). At each timepoint, high molecular weight HA in culture media was precipitated with CTAB and OD determined at a wavelength of 600 nm (Fig. 3B–D). We observed higher overall rates of HA degradation over the 24-hour period by $\chi 8768$ - and $\chi 8429$ -bHs (~ 0.15 OD units/hour), an intermediate rate for $\chi 8431$ -bHs (~ 0.10 OD units/hour; Supplementary Fig. S1E), and no degradation by SL7207-bHs, which recapitulates activity observed for each strain on HBL plates. The highest rate of degradation was observed for $\chi 8768$ -bHs during the first 12 hours of induction (~ 0.3 OD units/hour), whereas $\chi 8429$ -bHs and $\chi 8431$ -bHs showed two times less activity (~ 0.15 OD units/hour).

Ebelt et al.

**Figure 2.**

Growth kinetics and viability of bHs-expressing *Salmonella typhimurium* strains. OD readings (OD₆₀₀) for uninduced (solid blue circles) and induced (open red circles) *Salmonella typhimurium* strains SL7207 (A), χ 8429 (B), and χ 8768 (C) transformed with the pBAD-bHs construct. Cultures were done in triplicate and error bars represent SEM. D, Growth curves of induced bHs-expressing strains are compared. *, $P < 0.05$ by ANOVA. E, Bacterial cells from uninduced (-) and induced (+2% L-arabinose; L-ara) cultures of SL7207-bHs and χ 8768-bHs were stained at indicated time points (4 and 24 hours) with AO (live, green) and EB (dead, orange/red) and imaged by fluorescence microscopy at 100 \times magnification. Scale bar, 10 μ m. All data are representative of ≥ 3 experiments.

Overall, these data indicate that the χ 8768-bHs strain is most effective in degrading purified HA within hours of induction.

χ 8768-bHs effectively degrades tumor-derived HA

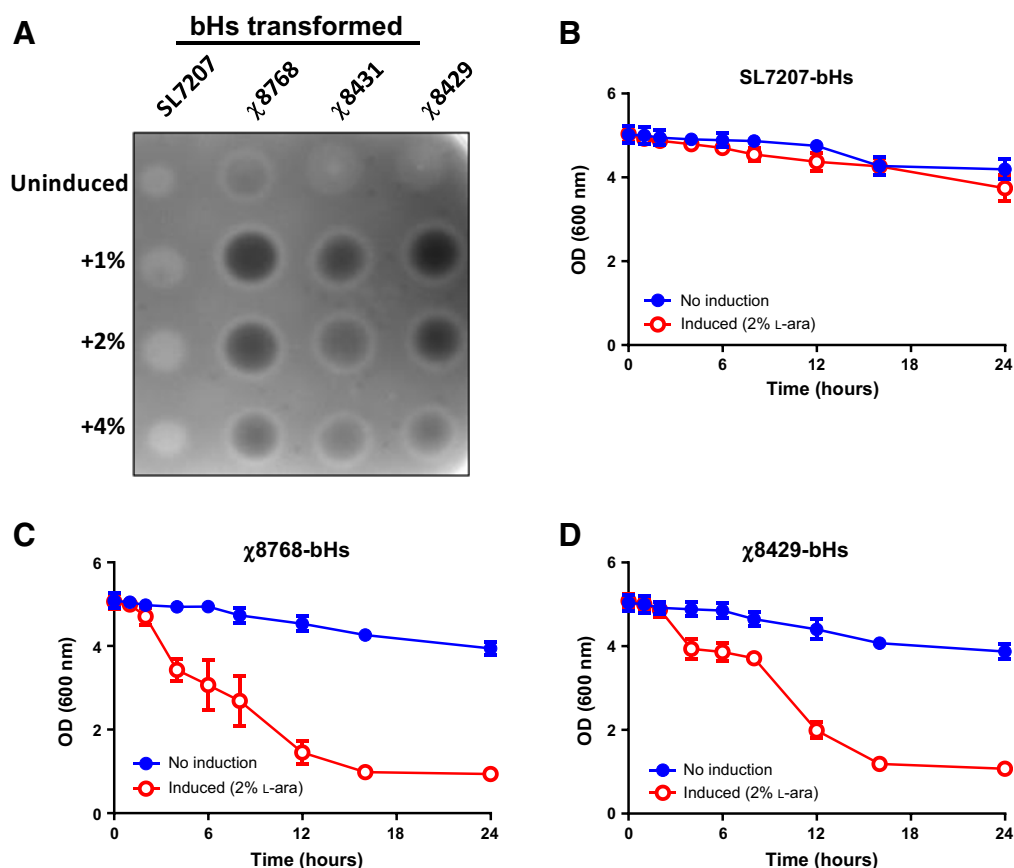
On the basis of its viability following induction and ability to efficiently degrade purified HA, we selected χ 8768-bHs to further determine whether bHs-expressing *Salmonella typhimurium* could degrade tumor-derived HA. We utilized the human pancreatic cancer line PANC-1, which we confirmed expresses high levels of HA when grown orthotopically in NSG (immune deficient) mice. We first performed *in vitro* HA degradation experiments, whereby fixed PANC-1 tumor sections were incubated with preinduced χ 8768-bHs. Overnight incubation of PANC-1 tumor sections with preinduced χ 8768-bHs resulted in dramatic degradation of HA compared with sections incubated with PBS or uninduced χ 8768-bHs (Fig. 4), with no observable loss or change in tumor cell content. We performed similar degradation experiments using the PC-3 prostate cancer cell line, which secretes high levels of HA while in culture, and also observed considerable depletion of HA by induced χ 8768-bHs with no change in tumor cell density (Supplementary Fig. S2). These results strongly suggest that χ 8768 expressing bHs degrades HA directly and not through a mechanism involving depletion of HA-expressing tumor cells.

Systemically delivered χ 8768-bHs degrades HA in xenograft PDAC tumors

We next determined the ability of χ 8768-bHs to colonize and deplete HA in orthotopically implanted PANC-1 tumors when deliv-

ered intravenously into mice. We first verified that the χ 8768 strain was capable of colonizing PANC-1 tumors utilizing a constitutive bacterial reporter gene construct encoding the bioluminescent LUX operon (44). When recombinant χ 8768 encoding LUX (χ 8768-LUX) was injected intravenously into NSG mice bearing orthotopically implanted PANC-1 tumors (>250 mm³), we observed bioluminescence localized to the area of the tumor, which was detected on day 3 and was undetectable on day 5 (Supplementary Fig. 3A). To further verify tumor-specific colonization by χ 8768-LUX, we isolated tumor, spleen, and liver (noted areas of *Salmonella typhimurium* accumulation; ref. 26) following intravenous injection and measured bioluminescence for each tissue type. Indeed, χ 8768-LUX was highly concentrated in tumor tissue, while completely absent in both spleen and liver (Supplementary Fig. 3B). These results suggest that χ 8768 is capable of colonizing orthotopic PANC-1 tumors after systemic administration and that tumor-specific colonization is achieved by day 2, which would represent an ideal timepoint for induction of bHs activity.

Thus, NSG mice with orthotopic PANC-1 tumors (>250 mm³) were intravenously administered 2.5×10^6 CFUs of χ 8768-bHs and then induced 2 days later by a single intraperitoneal injection of 240 mg of L-arabinose per mouse. PANC-1 tumors were excised 24 hours after induction and sectioned and stained for both HA and *Salmonella typhimurium*. As shown in Fig. 5A, tumors from mice receiving only χ 8768-bHs (uninduced) were characterized by limited (punctate) *Salmonella typhimurium* colonization and high HA deposition remaining in areas of *Salmonella typhimurium* colonization. In

Targeting Hyaluronan in PDAC using Recombinant *Salmonella***Figure 3.**

Functional analysis of bHs-expressing *Salmonella typhimurium* strains. **A**, bHs-expressing strains were cultured in LB media containing indicated percentages of L-arabinose for 3 hours at 37°C. A total of 1×10^8 CFUs were plated onto LB-hyaluronan-BSA agar plates overnight and then flushed with 2 N acetic acid. Plates were imaged on a black background to visualize areas of clearing, indicating hyaluronan breakdown. **B**, A total of 1×10^8 CFUs of ST-bHs strains were added to LB media containing 0% or 2% L-arabinose and 0.4 mg/mL HA. The CTAB turbidimetric method was used to determine rate of HA breakdown over 24 hours (OD₆₀₀) for pBAD-bHs-transformed SL7207, χ8768 (**C**) and χ8729 (**D**). Error bars, SEM. All data are representative of ≥ 3 experiments.

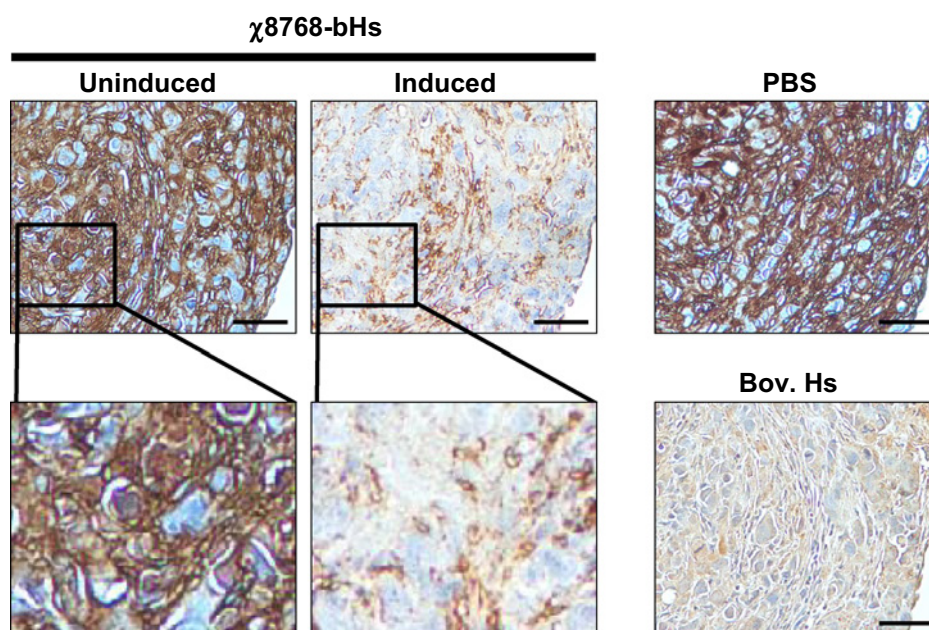
contrast, tumors from mice administered χ8768-bHs and L-arabinose (induced) showed a dramatic degradation of HA, particularly within areas colonized by χ8768-bHs (Fig. 5B), with no observable loss of tumor cell density based on DAPI (overlay) and pan-cytokeratin staining (Supplementary Fig. S3C). Remarkably, greater diffusion of χ8768-bHs ($P < 0.05$, t test) was also observed under induced conditions (Fig. 5C and D). We observed diffusion of χ8768-bHs from a number of duct-like structures into highly dense (DAPI positive) tumor tissue of induced mice, which were predominantly devoid of HA (Supplementary Fig. S3D). In uninduced mice, these structures were less prevalent but when observed, *Salmonella typhimurium* were found within the duct but had not diffused into the surrounding tissue, which displayed high HA staining. Similar to observations made *in vitro*, these *in vivo* results support a mechanism whereby HA depletion occurs predominantly through direct degradation by induced χ8768-bHs and not through reductions in tumor cell density. Through H&E staining, we identified vessel-like structures which are easily detected by the presence of red blood cells (Supplementary Fig. S3E). Tumors of induced mice displayed a predominance of larger, open vessel-like structures compared with a majority of smaller, closed structures in uninduced mice ($P <$

0.0001; t test; Supplementary Fig. S3F), reminiscent of the confined, punctate immunofluorescent staining of *Salmonella typhimurium* colonization in these tumors (Fig. 5C). Altogether, these data strongly suggest that χ8768-bHs is capable of effectively degrading tumor-derived HA *in vivo* to facilitate delivery of agents as large as *Salmonella typhimurium*, in which a single bacterium can measure 2.5 μm in width, 5 μm in length, and reach a molecular weight in the hundreds of gigadaltons (45–49).

χ8768-bHs potentiates the antitumor effects of gemcitabine treatment

We next evaluated the therapeutic benefits of HA degradation, by induced χ8768-bHs, when used in combination with gemcitabine chemotherapy. We utilized a subcutaneous PANC-1 xenograft model to measure tumor growth during treatment. We first confirmed the ability of χ8768-bHs to deplete HA in subcutaneous PANC-1 tumors and also determined the duration of HA depletion following induction. As shown in Fig. 6A, we observed a greater presence of χ8768-bHs and specific depletion of HA in PANC-1 tumors 3 and 7 days after induction that is not present under uninduced conditions or in other HA-rich tissues, such as the skin and joints (Supplementary Fig. S4A),

Ebelt et al.

**Figure 4.**

Induced χ 8768-bHs effectively depletes tumor-derived hyaluronan. χ 8768-bHs was grown for 3 hours in LB media containing 0% (uninduced) or 2% (induced) L-arabinose. A total of 1×10^8 CFUs were then coincubated with deparaffinized serial sections of PANC-1 tumor tissue overnight. HA was detected using biotinylated HABP followed by incubation with streptavidin-HRP and ImmPACT DAB substrate. Serial sections incubated with PBS serve as an HA-positive control, and specificity of HABP was confirmed through overnight incubation with 10 U/mL bovine hyaluronidase (Bov Hs). Scale bar, 75 μ m. All images are representative of ≥ 3 experiments.

under induced conditions. Only minimal punctate χ 8768-bHs tumor colonization was observed on day 3 under uninduced conditions, which is completely absent by day 7 and on day 14 (Fig. 6A; Supplementary Fig. S4B). However, under induced conditions, χ 8768-bHs and HA depletion were still present in PANC-1 tumors on day 7 and waned by day 14. Similar to previous observations, there was no loss of tumor cell density (based on pan-cytokeratin and DAPI staining) or collagen degradation (trichrome) in HA-depleted areas (Supplementary Fig. S4B and S4C). These data suggest that systemically delivered χ 8768-bHs is capable of depleting HA specifically in PANC-1 tumors for an extended period following induction.

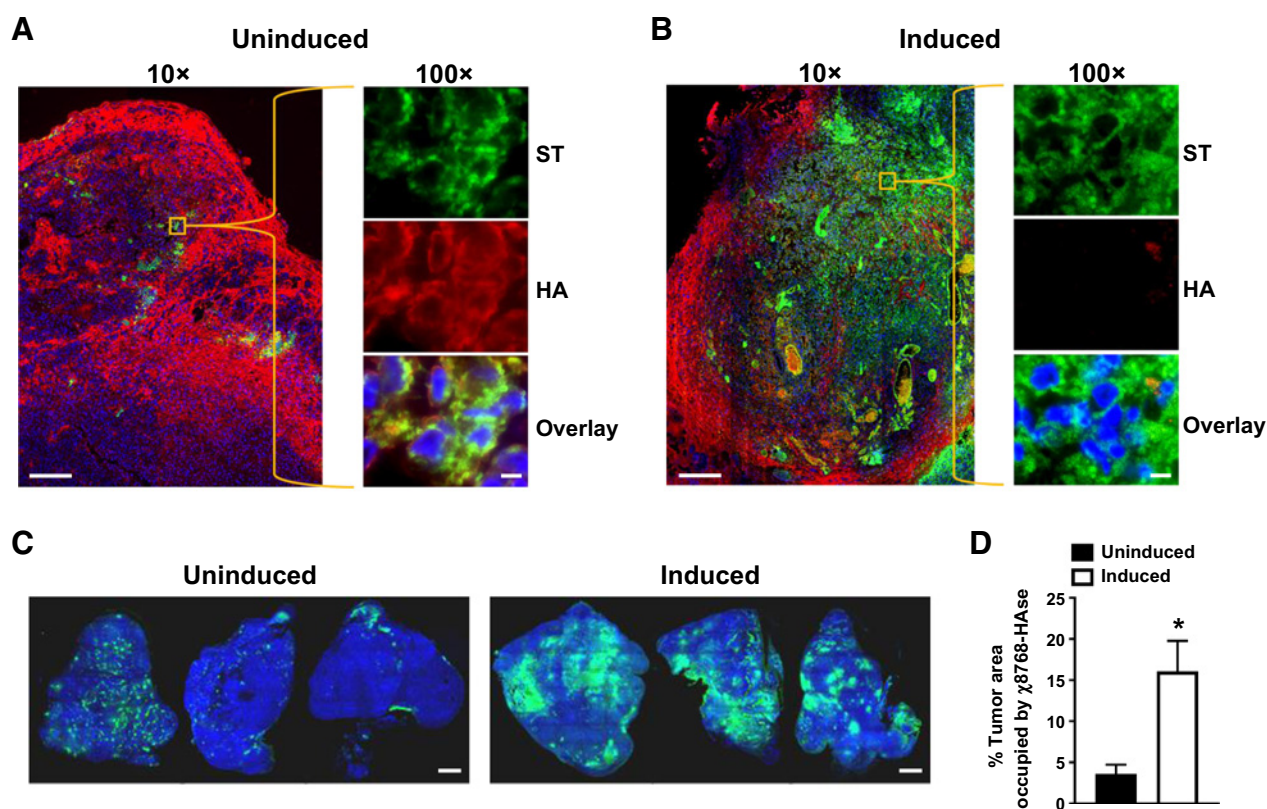
We next determined whether HA depletion by induced χ 8768-bHs could improve the efficacy of gemcitabine in the PANC-1 model. Mice with established subcutaneous PANC-1 tumors ($n = 6$; $>150 \text{ mm}^3$) were administered χ 8768-bHs and were induced or left uninduced 48 hours later by intraperitoneal injection of L-arabinose or PBS, respectively. For mice receiving gemcitabine, 40 mg/kg were administered 2 days postintra-peritoneal injection (dpi) and twice per week thereafter. As shown in Fig. 6B, tumor growth rates for mice having received induced χ 8768-bHs in combination with gemcitabine were significantly reduced (weeks 9–11; $P < 0.01, 0.001$; ANOVA) compared with groups receiving χ 8768-bHs alone or uninduced χ 8768-bHs in combination with gemcitabine. In addition, no significant change from initial body weight was observed in mice receiving χ 8768-bHs alone compared with PBS (Fig. 6C). Only negligible weight loss ($<10\%$) was observed in groups receiving gemcitabine, with no discernable added weight loss caused by χ 8768-bHs pretreatment under induced conditions. Overall, these data indicate that χ 8768-bHs treatment can deplete HA in tumors for an extended period of time to improve efficacy of gemcitabine with little to no added toxicity.

Discussion

Hyaluronidase administration has been shown to enhance the efficacy of gemcitabine and nAb-paclitaxel in PDAC tumor models and has had some clinical benefit in patients with PDAC (15, 50). However, the high risk of adverse effects associated with systemically

delivered hyaluronidase still presents major concerns due to ECM degradation in healthy tissues. To reduce risk, lower doses of hyaluronidase must be given, which may not necessarily maximize the therapeutic efficacy of chemotherapy. BHs-ST is the first example of a microbial-based, ECM-degrading agent that focuses its enzymatic activity strictly to tumor tissue, potentially maximizing HA degradation and therapeutic drug delivery. We established that bHs is anchored to the surface of *Salmonella typhimurium*, reducing the likelihood of systemic off-tumor effects resulting from circulating bHs. Previous studies have also shown that bHs expressed by *S. koganeinsis* has a unique specificity to HA, further reducing the risk of degrading other major ECM components in healthy tissue. Furthermore, we and others have shown replication of attenuated *Salmonella typhimurium* in tumor tissue, suggesting that an initial input of bHs-ST could be amplified in tumors for a few days, before induction of bHs expression, to cause maximal HA degradation and minimal off-target effects. The ability of attenuated *Salmonella typhimurium* to extensively and preferentially colonize tumors also increases the window for therapeutic intervention and delivery. The types and sizes of therapeutic agents that show enhanced delivery and whether multiple administrations are possible will be ongoing studies to determine the overall utility of bHs-ST. For greater feasibility, an autonomous version of bHs-*Salmonella typhimurium* will likely need to be developed to avoid additional induction steps. Furthermore, transient tumor colonization by *Salmonella typhimurium*, as observed in Fig. 6A and Supplementary Fig. S3A, would be a limitation of our current strategy, requiring multiple doses and/or exquisite timing of induction for optimal HA depletion in each individual. The use of tumor-specific promoters, such as hypoxia-inducible promoters, to drive bHs expression is one potential solution to overcome this (51).

In some cases, *Salmonella typhimurium*-based cancer therapy has been shown to regress tumors in preclinical models, and this regression is heavily dependent on the ability of *Salmonella typhimurium* to colonize tumors (52, 53). The first attenuated *Salmonella typhimurium* to enter clinical trials, VNP20009, was administered to patients with metastatic melanoma and head and neck cancer (25). Virtually no tumor regression was observed in any patients receiving VNP20009,

**Figure 5.**

Systemic delivery of χ 8768-bHs effectively degrades HA within xenograft PANC-1 tumors. Uninduced χ 8768-bHs (2.5×10^6 CFU) was injected intravenously into NSG mice bearing orthotopic PANC-1 tumors ($>250 \text{ mm}^3$). After 48 hours, mice were then administered PBS (uninduced; **A**) or 240 mg L-arabinose (induced; **B**) by intraperitoneal injection. Tumors were isolated 16 hours later, sectioned and stained for *Salmonella typhimurium* (ST; green) and HA (red) for subsequent IF imaging at 10 \times and 100 \times magnification. Blue, nuclear staining using DAPI. 10 \times scale bars, 200 μm ; 100 \times scale bars, 10 μm . **C**, Tile scanning was performed on entire tumor sections at 10 \times magnification. Sections were stained for *Salmonella typhimurium* (green) and DAPI (blue) for subsequent IF imaging. Scale bars, 2 mm. Representative tumors are shown for uninduced and induced groups. **D**, Percent area of tumor colonized by χ 8768-Hase under uninduced and induced conditions based on IF. Percentage calculated using the following: [area occupied by χ 8768-Hase (green)/total tumor area (DAPI)] \times 100%. Areas (μm^2) were determined using Image-Pro Plus (Media Cybernetics) analysis software. *, $P < 0.05$; t test. All data are representative of ≥ 3 experiments.

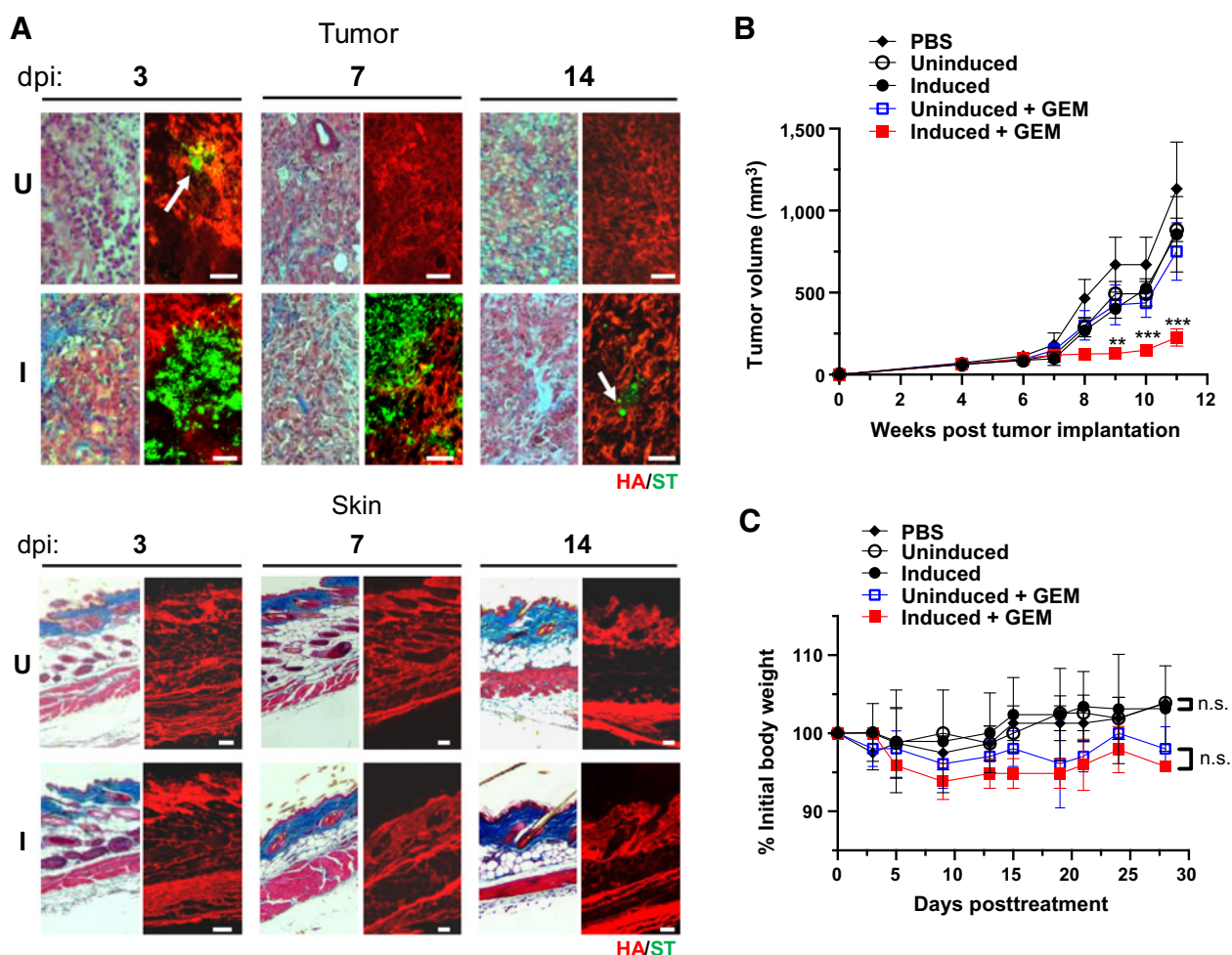
and only a small number of patients had tumors colonized by *Salmonella typhimurium*. Our ability to express bHs in *Salmonella typhimurium* could significantly increase tumor colonization, as shown for induced bHs-ST, and could potentially increase efficacy of *Salmonella typhimurium*-based therapies. In this study, increased distribution of induced χ 8768-bHs within PANC-1 tumors was not shown to be therapeutic alone, which is likely a limitation of using an immunocompromised xenograft model. Indeed, previous work utilizing PEGPH20 in immunocompetent mice significantly improved colonization and antitumor efficacy of our *Salmonella typhimurium*-based therapeutic targeting indoleamine 2,3-dioxygenase (shIDO-ST; ref. 23). Thus, χ 8768-bHs alone could prove to be more tumor-specific and therapeutic, compared with hyaluronidase, in an immunocompetent setting (17). Overall, these observations suggest that delivery of relatively large particles such as bacteria could be enhanced through the use of ECM-degrading enzymes. Therefore, bHs-ST pretreatment could easily be combined with virotherapy, cell- or antibody-based therapies to improve their delivery.

In addition to increasing interstitial fluidic pressure, which prevents blood flow and diffusion of therapeutic agents, HA also plays a large part in tumor progression as a signaling molecule that activates intracellular pathways and promotes motility and metastasis (54, 55).

Indeed, clinical data reveal a better prognosis for patients with lower deposition of HA (8, 10). Thus, targeting HA alone may be sufficient to cause primary tumor regression as seen in PC3 prostate tumors (56) or prevent metastasis. However, preclinical and clinical trials have shown that targeting hyaluronan alone does little to decrease tumor growth and metastasis (7, 57). A few key studies in PDAC have even shown that ECM depletion may be detrimental to overall survival as the ECM may act as a physical barrier to tumor cell dissemination, and the increased vascularization can increase tumor cell survival (58). Thus, the beneficial effect of hyaluronidase treatment for tumors will be in its ability to improve delivery of therapeutic drugs or antibodies (57), and for PDAC, the aforementioned data may indicate that ECM depletion must go hand-in-hand with chemotherapy or other anticancer treatment to avoid possible unfavorable effects.

The number of therapies being developed to treat cancer, which includes nanoparticles, antibody-based therapies, chemotherapeutic combinations, viruses and bacteria, and T-cell therapies, continues to rise and, therefore, strategies to improve penetration of these agents is also required. Currently, only a small number of ECM-targeting agents can claim to improve intratumoral drug delivery, with the caveat of systemic ECM degradation and associated adverse events (7, 14). We have developed an ECM-degrading agent that is more tumor-specific

Ebelt et al.

**Figure 6.**

χ 8768-bHs potentiates the antitumor effects of gemcitabine (GEM) treatment in PANC-1 tumor xenografts. Uninduced χ 8768-bHs (2.5×10^6 CFU) was injected i.v. into NSG mice bearing subcutaneous PANC-1 tumors ($>150 \text{ mm}^3$). After 48 hours, mice were then administered PBS (uninduced, U) or 240 mg L-arabinose (induced, I) by i.p. injection. **A**, Subcutaneous tumors and skin ($n = 4$) were isolated 3, 7, and 11 dpi, sectioned, and stained for HA (red) and *Salmonella typhimurium* (green) for subsequent IF imaging at $5\times$ magnification. Trichrome staining of serial sections for same tissue sample also shown to left of IF images. Representative images shown. Arrows indicate area of *Salmonella typhimurium* (ST)/HA overlap. Scale bars, 50 μm . **B**, After 2 dpi, groups of tumor-bearing mice ($n = 6$) were administered either gemcitabine (40 mg/kg) or diluent control (0.9% saline) by intraperitoneal route, followed by additional administrations twice per week. PBS-only group did not receive pretreatment with χ 8768-bHs. Tumors were measured weekly using a digital caliper. **, $P < 0.01$; ***, $P < 0.001$; ANOVA with Tukey *post hoc* test. **C**, Mouse body weights were measured on indicated days following gemcitabine or control treatment and are presented as a percentage of initial body weight. n.s., not significant.

and, thus, can increase the number of potential therapeutic combinations to maximize efficacy while minimizing toxicity. In this work, we show that bHs-ST is capable of targeting tumor-derived HA in PDAC tumors and increases penetration of large particles. While bHs-ST may only be effective in patients with HA-high tumors, such as those selected for treatment with PEGPH20 (50), the *Salmonella typhimurium* platform described in this work could be used to develop other ECM-targeting strategies with more universal application and benefit to patients with PDAC.

Disclosure of Potential Conflicts of Interest

No potential conflicts of interest were disclosed.

Disclaimer

The content is solely the responsibility of the authors and does not necessarily represent the official views of the National Institutes of Health.

Authors' Contributions

Conception and design: N.D. Ebelt, E.R. Manuel

Development of methodology: N.D. Ebelt, E. Zuniga, E.R. Manuel

Acquisition of data (provided animals, acquired and managed patients, provided facilities, etc.): N.D. Ebelt, E. Zuniga, K.B. Passi, L.J. Sobocinski, E.R. Manuel

Analysis and interpretation of data (e.g., statistical analysis, biostatistics, computational analysis): N.D. Ebelt, E.R. Manuel

Writing, review, and/or revision of the manuscript: N.D. Ebelt, E.R. Manuel

Targeting Hyaluronan in PDAC using Recombinant *Salmonella*

Administrative, technical, or material support (i.e., reporting or organizing data, constructing databases): N.D. Ebelt, E. Zuniga, K.B. Passi, L.J. Sobocinski, E.R. Manuel

Study supervision: E.R. Manuel

Acknowledgments

Research reported in this article included work performed in the Molecular Pathology, Animal Resource Center, Small Animal Imaging, and Light Microscopy

Digital Imaging cores supported by the NCI of the NIH under grant number P30CA033572.

The costs of publication of this article were defrayed in part by the payment of page charges. This article must therefore be hereby marked *advertisement* in accordance with 18 U.S.C. Section 1734 solely to indicate this fact.

Received May 28, 2019; revised September 9, 2019; accepted October 29, 2019; published first November 6, 2019.

References

- Lee JJ, Huang J, England CG, McNally LR, Frieboes HB. Predictive modeling of in vivo response to gemcitabine in pancreatic cancer. *PLoS Comput Biol* 2013;9:e1003231.
- Conroy T, Hammel P, Hebbar M, Ben Abdelghani M, Wei ACC, Raoul JL, et al. Unicancer GI PRODIGE 24/CCTG PA.6 trial: a multicenter international randomized phase III trial of adjuvant mFOLFIRINOX versus gemcitabine (gem) in patients with resected pancreatic ductal adenocarcinomas. *J Clin Oncol* 2018;36:18 Suppl.
- Taberero J, Chiorean EG, Infante JR, Hingorani SR, Ganju V, Weekes C, et al. Prognostic factors of survival in a randomized phase III trial (MPACT) of weekly nab-paclitaxel plus gemcitabine versus gemcitabine alone in patients with metastatic pancreatic cancer. *Oncologist* 2015;20:143–50.
- Han H, Von Hoff DD. SnapShot: pancreatic cancer. *Cancer Cell* 2013;23:424.
- Sirri E, Castro FA, Kieschke J, Jansen L, Emrich K, Gondos A, et al. Recent trends in survival of patients with pancreatic cancer in Germany and the United States. *Pancreas* 2016;45:908–14.
- Erkan M, Hausmann S, Michalski CW, Fingerle AA, Dobritz M, Kleeff J, et al. The role of stroma in pancreatic cancer: diagnostic and therapeutic implications. *Nat Rev Gastroenterol Hepatol* 2012;9:454–67.
- Jacobetz MA, Chan DS, Neesse A, Bapiro TE, Cook N, Frese KK, et al. Hyaluronan impairs vascular function and drug delivery in a mouse model of pancreatic cancer. *Gut* 2013;62:112–20.
- Auvinen P, Rilla K, Tumelius R, Tammi M, Sironen R, Soini Y, et al. Hyaluronan synthases (HAS1–3) in stromal and malignant cells correlate with breast cancer grade and predict patient survival. *Breast Cancer Res Treat* 2014;143:277–86.
- Josefsson A, Adamo H, Hammarsten P, Granfors T, Stattin P, Egevad L, et al. Prostate cancer increases hyaluronan in surrounding nonmalignant stroma, and this response is associated with tumor growth and an unfavorable outcome. *Am J Pathol* 2011;179:1961–8.
- Whatcott CJ, Diep CH, Jiang P, Watanabe A, LoBello J, Sima C, et al. Desmoplasia in primary tumors and metastatic lesions of pancreatic cancer. *Clin Cancer Res* 2015;21:3561–8.
- Huang H, Brekken RA. The next wave of stroma-targeting therapy in pancreatic cancer. *Cancer Res* 2019;79:328–30.
- Cun X, Ruan S, Chen J, Zhang L, Li J, He Q, et al. A dual strategy to improve the penetration and treatment of breast cancer by combining shrinking nanoparticles with collagen depletion by losartan. *Acta Biomater* 2016;31:186–96.
- Schuster L, Seifert O, Vollmer S, Kontermann RE, Schlosshauer B, Hartmann H. Immunoliposomes for targeted delivery of an antifibrotic drug. *Mol Pharm* 2015;12:3146–57.
- Elahi-Gedwillo KY, Carlson M, Zettervall J, Provenzano PP. Antifibrotic therapy disrupts stromal barriers and modulates the immune landscape in pancreatic ductal adenocarcinoma. *Cancer Res* 2019;79:372–86.
- Hingorani SR, Zheng L, Bullock AJ, Seery TE, Harris WP, Sigal DS, et al. HALO 202: randomized phase II study of PEGPH20 plus nab-paclitaxel/gemcitabine versus nab-paclitaxel/gemcitabine in patients with untreated, metastatic pancreatic ductal adenocarcinoma. *J Clin Oncol* 2018;36:359–66.
- Baumgartner G, Gomar-Hoss C, Sakr L, Ulsperger E, Wogritsch C. The impact of extracellular matrix on the chemoresistance of solid tumors—experimental and clinical results of hyaluronidase as additive to cytostatic chemotherapy. *Cancer Lett* 1998;131:85–99.
- Beckenlehner K, Bannek S, Spruss T, Bernhardt G, Schonenberg H, Schiess W. Hyaluronidase enhances the activity of adriamycin in breast cancer models in vitro and in vivo. *J Cancer Res Clin Oncol* 1992;118:591–6.
- Guedan S, Rojas JJ, Gros A, Mercade E, Cascallo M, Alemany R. Hyaluronidase expression by an oncolytic adenovirus enhances its intratumoral spread and suppresses tumor growth. *Mol Ther* 2010;18:1275–83.
- Hoffman P, Meyer K, Linker A. Transglycosylation during the mixed digestion of hyaluronic acid and chondroitin sulfate by testicular hyaluronidase. *J Biol Chem* 1956;219:653–63.
- Stern R, Jedrzejas MJ. Hyaluronidases: their genomics, structures, and mechanisms of action. *Chem Rev* 2006;106:818–39.
- Pavan M, Beninato R, Galesso D, Panfilo S, Vaccaro S, Messina L, et al. A new potential spreading factor: *Streptomyces koganeiensis* hyaluronidase. A comparative study with bovine testes hyaluronidase and recombinant human hyaluronidase of the HA degradation in ECM. *Biochim Biophys Acta* 2016;1860:661–8.
- Hynes WL, Walton SL. Hyaluronidases of Gram-positive bacteria. *FEMS Microbiol Lett* 2000;183:201–7.
- Manuel ER, Chen J, D'Apuzzo M, Lampa MG, Kaltcheva TI, Thompson CB, et al. Salmonella-based therapy targeting indoleamine 2,3-dioxygenase coupled with enzymatic depletion of tumor hyaluronan induces complete regression of aggressive pancreatic tumors. *Cancer Immunol Res* 2015;3:1096–107.
- Jia LJ, Xu HM, Ma DY, Hu QG, Huang XF, Jiang WH, et al. Enhanced therapeutic effect by combination of tumor-targeting Salmonella and endostatin in murine melanoma model. *Cancer Biol Ther* 2005;4:840–5.
- Toso JF, Gill VJ, Hwu P, Marincola FM, Restifo NP, Schwartzentruber DJ, et al. Phase I study of the intravenous administration of attenuated *Salmonella typhimurium* to patients with metastatic melanoma. *J Clin Oncol* 2002;20:142–52.
- Pawelek JM, Low KB, Bermudes D. Tumor-targeted *Salmonella* as a novel anticancer vector. *Cancer Res* 1997;57:4537–44.
- Orlando Z, Lengens I, Melzig MF, Buschauer A, Hensel A, Jose J. Autodisplay of human hyaluronidase Hyal-1 on *Escherichia coli* and identification of plant-derived enzyme inhibitors. *Molecules* 2015;20:15449–68.
- Kaessler A, Olgen S, Jose J. Autodisplay of catalytically active human hyaluronidase hPH-20 and testing of enzyme inhibitors. *Eur J Pharm Sci* 2011;42:138–47.
- Hofinger ES, Spickenreither M, Oschmann J, Bernhardt G, Rudolph R, Buschauer A. Recombinant human hyaluronidase Hyal-1: insect cells versus *Escherichia coli* as expression system and identification of low molecular weight inhibitors. *Glycobiology* 2007;17:444–53.
- Uphoff CC, Drexler HG. Detecting *Mycoplasma* contamination in cell cultures by polymerase chain reaction. *Methods Mol Med* 2004;88:319–26.
- Bollen WS, Gunn BM, Mo H, Lay MK, Curtiss R III. Presence of wild-type and attenuated *Salmonella enterica* strains in brain tissues following inoculation of mice by different routes. *Infect Immun* 2008;76:3268–72.
- Xiong G, Hussein MI, Song L, Erdreich-Epstein A, Shackelford GM, Seeger RC, et al. Novel cancer vaccine based on genes of *Salmonella* pathogenicity island 2. *Int J Cancer* 2010;126:2622–34.
- Hoiseth SK, Stocker BA. Aromatic-dependent *Salmonella typhimurium* are non-virulent and effective as live vaccines. *Nature* 1981;291:238–9.
- Evans DT, Chen LM, Gillis J, Lin KC, Harty B, Mazzara GP, et al. Mucosal priming of simian immunodeficiency virus-specific cytotoxic T-lymphocyte responses in rhesus macaques by the *Salmonella* type III secretion antigen delivery system. *J Virol* 2003;77:2400–9.
- Johnson SA, Ormsby MJ, Wall DM. Draft genome sequence of the tumor-targeting *Salmonella enterica* serovar Typhimurium strain SL7207. *Genome Announc* 2017;5:e01591–16.
- Oueslati N, Leblanc P, Harscoat-Schiavo C, Rondags E, Meunier S, Kapel R, et al. CTAB turbidimetric method for assaying hyaluronic acid in complex environments and under cross-linked form. *Carbohydr Polym* 2014;112:102–8.
- Tseng WW, Winer D, Kenkel JA, Choi O, Shain AH, Pollack JR, et al. Development of an orthotopic model of invasive pancreatic cancer in an immunocompetent murine host. *Clin Cancer Res* 2010;16:3684–95.

Ebelt et al.

38. Guzman LM, Belin D, Carson MJ, Beckwith J. Tight regulation, modulation, and high-level expression by vectors containing the arabinose PBAD promoter. *J Bacteriol* 1995;177:4121–30.
39. Matusiak M, Van Opdenbosch N, Vande Walle L, Sirard JC, Kanneganti TD, Lamkanfi M. Flagellin-induced NLRC4 phosphorylation primes the inflammatory for activation by NAIP5. *Proc Natl Acad Sci U S A* 2015;112:1541–6.
40. Chou KC, Shen HB. Cell-PLoc: a package of Web servers for predicting subcellular localization of proteins in various organisms. *Nat Protoc* 2008;3:153–62.
41. Yu NY, Laird MR, Spencer C, Brinkman FS. PSORTdb—an expanded, auto-updated, user-friendly protein subcellular localization database for bacteria and archaea. *Nucleic Acids Res* 2011;39:D241–4.
42. Tusnady GE, Simon I. The HMMTOP transmembrane topology prediction server. *Bioinformatics* 2001;17:849–50.
43. Kasibhatla S, Amarante-Mendes GP, Finucane D, Brunner T, Bossy-Wetzel E, Green DR. Acridine orange/ethidium bromide (AO/EB) staining to detect apoptosis. *CSH Protoc* 2006;2006. doi: 10.1101/pdb.prot4493.
44. Karsi A, Lawrence ML. Broad host range fluorescence and bioluminescence expression vectors for Gram-negative bacteria. *Plasmid* 2007;57:286–95.
45. Weniger M, Honselmann KC, Liss AS. The extracellular matrix and pancreatic cancer: a complex relationship. *Cancers* 2018;10. doi: 10.3390/cancers10090316.
46. DuFort CC, DelGiorno KE, Carlson MA, Osgood RJ, Zhao C, Huang Z, et al. Interstitial pressure in pancreatic ductal adenocarcinoma is dominated by a gel-fluid phase. *Biophys J* 2016;110:2106–19.
47. Chauhan VP, Boucher Y, Ferrone CR, Roberge S, Martin JD, Stylianopoulos T, et al. Compression of pancreatic tumor blood vessels by hyaluronan is caused by solid stress and not interstitial fluid pressure. *Cancer Cell* 2014;26:14–5.
48. Provenzano PP, Hingorani SR. Hyaluronan, fluid pressure, and stromal resistance in pancreas cancer. *Br J Cancer* 2013;108:1–8.
49. Fabrega A, Vila J. Salmonella enterica serovar Typhimurium skills to succeed in the host: virulence and regulation. *Clin Microbiol Rev* 2013;26:308–41.
50. Doherty GJ, Tempero M, Corrie PG. HALO-109-301: a phase III trial of PEGPH20 (with gemcitabine and nab-paclitaxel) in hyaluronic acid-high stage IV pancreatic cancer. *Future Oncol* 2018;14:13–22.
51. Mengesha A, Dubois L, Lambin P, Landuyt W, Chiu RK, Wouters BG, et al. Development of a flexible and potent hypoxia-inducible promoter for tumor-targeted gene expression in attenuated Salmonella. *Cancer Biol Ther* 2006;5:1120–8.
52. Felgner S, Kocijancic D, Frahm M, Heise U, Rohde M, Zimmermann K, et al. Engineered Salmonella enterica serovar Typhimurium overcomes limitations of anti-bacterial immunity in bacteria-mediated tumor therapy. *Oncoimmunology* 2018;7:e1382791.
53. Yu B, Shi L, Zhang BZ, Zhang KE, Peng X, Niu HB, et al. Obligate anaerobic Salmonella typhimurium strain YB1 treatment on xenograft tumor in immunocompetent mouse model. *Oncol Lett* 2015;10:1069–74.
54. Cheng XB, Kohi S, Koga A, Hirata K, Sato N. Hyaluronan stimulates pancreatic cancer cell motility. *Oncotarget* 2015;7:4829–40.
55. Cheng XB, Sato N, Kohi S, Koga A, Hirata K. Receptor for hyaluronic acid-mediated motility is associated with poor survival in pancreatic ductal adenocarcinoma. *J Cancer* 2015;6:1093–8.
56. Thompson CB, Shepard HM, O'Connor PM, Kadhim S, Jiang P, Osgood RJ, et al. Enzymatic depletion of tumor hyaluronan induces antitumor responses in preclinical animal models. *Mol Cancer Ther* 2010;9:3052–64.
57. Infante JR, Korn RL, Rosen LS, LoRusso P, Dychter SS, Zhu J, et al. Phase 1 trials of PEGylated recombinant human hyaluronidase PH20 in patients with advanced solid tumours. *Br J Cancer* 2017;118:153.
58. Rhim AD, Oberstein PE, Thomas DH, Mirek ET, Palermo CF, Sastra SA, et al. Stromal elements act to restrain, rather than support, pancreatic ductal adenocarcinoma. *Cancer Cell* 2014;25:735–47.

Molecular Cancer Therapeutics

Hyaluronidase-Expressing *Salmonella* Effectively Targets Tumor-Associated Hyaluronic Acid in Pancreatic Ductal Adenocarcinoma

Nancy D. Ebel, Edith Zuniga, Kevin B. Passi, et al.

Mol Cancer Ther 2020;19:706-716. Published OnlineFirst November 6, 2019.

Updated version Access the most recent version of this article at:
[doi:10.1158/1535-7163.MCT-19-0556](https://doi.org/10.1158/1535-7163.MCT-19-0556)

Supplementary Material Access the most recent supplemental material at:
<http://mct.aacrjournals.org/content/suppl/2019/11/06/1535-7163.MCT-19-0556.DC1>

Cited articles This article cites 55 articles, 16 of which you can access for free at:
<http://mct.aacrjournals.org/content/19/2/706.full#ref-list-1>

E-mail alerts [Sign up to receive free email-alerts](#) related to this article or journal.

Reprints and Subscriptions To order reprints of this article or to subscribe to the journal, contact the AACR Publications Department at pubs@aacr.org.

Permissions To request permission to re-use all or part of this article, use this link
<http://mct.aacrjournals.org/content/19/2/706>.
Click on "Request Permissions" which will take you to the Copyright Clearance Center's (CCC) Rightslink site.